Equilibrium and Kinetic Unfolding Properties of Dimeric Human Glutathione Transferase A1-1[†]

Louise A. Wallace, Nicolas Sluis-Cremer, and Heini W. Dirr*

Department of Biochemistry, University of the Witwatersrand, Johannesburg 2050, South Africa

Received December 2, 1997; Revised Manuscript Received February 5, 1998

ABSTRACT: The equilibrium and kinetic unfolding properties of homodimeric class α glutathione transferase (hGST A1-1) were characterized. Urea-induced equilibrium unfolding data were consistent with a folded dimer/unfolded monomer transition. Unfolding kinetics were investigated, using stopped-flow fluorescence, as a function of denaturant concentration (3.5−8.9 M urea) and temperature (10−40 °C). The unfolding pathway, monitored by tryptophan fluorescence, was biphasic with a fast unfolding event (millisecond time range with enhanced fluorescence properties) and a slow unfolding event (seconds to minutes time range with quenched fluorescence properties). Both events occurred simultaneously from 3.5 M urea. Each phase displayed single-exponential behavior, consistent with two unimolecular reactions. Urea-dependence studies and thermodynamic activation parameters (transition-state theory) suggest that the transition state for each phase is well-structured and is closely related to native protein in terms of solvent exposure. The apparent activation Gibbs free energy change in the absence of denaturant, $\Delta G^{\ddagger}(H_2O)$, indicates that the slow unfolding event represents the transition state for the overall unfolding pathway. The rate and urea independence of each phase on the initial condition exclude the possibility of a preexisting equilibrium between various native forms in the pretransition baseline. The unfolding pathways monitored by energy transfer to or direct excitation of AEDANS covalently linked to Cys111 in hGST A1-1 were monophasic with urea and temperature properties similar to those observed for the slow unfolding event (described above). A sequential unfolding kinetic mechanism involving the partial dissociation of the two structurally distinct domains per subunit followed by complete domain and subunit unfolding is proposed.

The folding of a protein into its unique three-dimensional conformation utilizes the information contained in its linear amino acid sequence (*1*). Folding of a protein is crucial to its role in the cell since the biochemical character of a protein is determined by its three-dimensional state. The complete folding pathway of a protein is characterized by both the folding and the unfolding pathways, the transient formation of intermediates, and the transition states between the native and unfolded states (*2*). The investigations of protein folding have primarily used small monomeric proteins as model systems (*3*, *4*). However, the use in applying these to understand the folding mechanism of dimeric/oligomeric proteins is ambiguous.

The folding/unfolding pathway for oligomeric proteins has been addressed using the P22 Arc repressor (*5*), the *Escherichia coli Trp* aporepressor (*6*, *7*), the gene V protein of bacteriophage (*8*), and the β subunit of tryptophan synthase (*9*). In addition, several NMR studies have been performed on the denatured state of proteins to structurally characterize the unfolded species and any molecular interactions that may affect the protein folding pathway (*10*).

The equilibrium and kinetic unfolding pathways of the homodimeric human class α glutathione transferase (hGST A1-1)[1] were investigated in this study. Cytosolic glutathione transferases (EC 2.5.1.18) are a supergene family of multifunctional proteins which can be classified into one of six species-independent gene classes: α, μ, π (*11*), σ (*12*), θ (*13*), and κ (*14*). All cytosolic glutathione transferases exist as stable homo- or heterodimeric structures ($M_r \approx 50$ kDa), and three-dimensional representatives from these classes show similar archetypical folds (for reviews, see refs *15* and *16*). In the cell, the glutathione transferases function in cell detoxification using the mercapturate pathway and in ligand binding of many hydrophobic xenobiotic compounds (*17*).

hGST A1-1 is a homodimer of identical subunits of 221 amino acids each (Figure 1) (*18*). Each subunit is composed of two structurally distinct domains: an N-terminal α/β domain (81 residues) and a C-terminal all α-helical domain (140 residues). Fifteen residues of the C-terminus (the α

[†] This work was supported by the University of the Witwatersrand and the South African Foundation for Research and Development (FRD).

* Correspondence should be addressed to this author at the Protein Structure−Function Research Program. E-mail: 089dirr@cosmos.wits.ac.za.

[1] Abbreviations: AEDANS, 5-[[2-(acetylamino)ethyl]amino]naphthalene-1-sulfonic acid; ANS, 8-anilino-1-naphthalenesulfonate; DSC, differential scanning calorimetry; $\Delta G^{\ddagger}(T_o)$, $\Delta H^{\ddagger}(T_o)$, $\Delta S^{\ddagger}(T_o)$, thermodynamic activation parameters at standard temperature (298 K); hGST A1-1, human class α-glutathione transferase with two type 1 subunits; IAEDANS, 5-[[2-[(iodoacetyl)amino]ethyl]amino]naphthalene-1-sulfonic acid; k_u, first-order rate constant for unfolding; NATA, *N*-acetyl-L-tryptophanamide; SASA, solvent-accessible surface area; SEC−HPLC, size exclusion chromatography−high-performance liquid chromatography.

S0006-2960(97)02936-X CCC: $15.00
Published on Web 03/20/1998

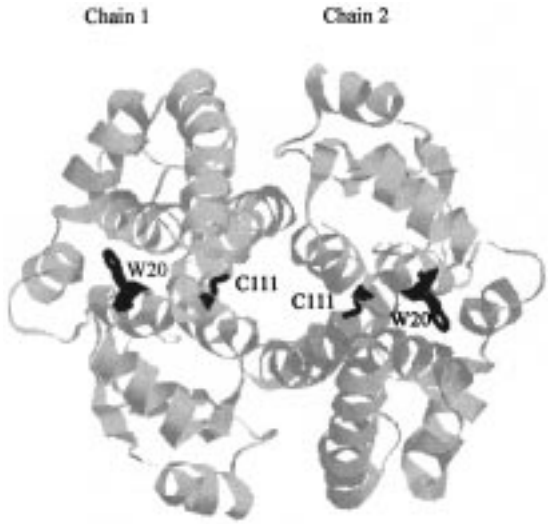

FIGURE 1: Cartoon representative of the structure of dimeric human glutathione transferase A1-1 (*18*) parallel to the 2-fold axis. The structuring of the α helix 9 over the H-site and the side chains of Trp20 and Cys111 are indicated.

helix 9) form part of the hydrophobic electrophile-binding site. This structural feature is unique to the α-class and provides a "lid" over the active site in the presence of ligands (*19*). In ligand-free hGST A1-1, the α helix 9 is conformationally flexible (*20*). The dimeric structure of the glutathione transferases is required for formation of two active sites (the H-site and G-site) per subunit and formation of the nonsubstrate ligand-binding site (L-site) at the dimer interface.

In this paper, the equilibrium unfolding and dissociation of hGST A1-1 reported was consistent with the two-state pathway involving the native dimer and unfolded monomer as previously shown for the class π (pGST P1-1) and *Schistosoma japonicum* (sj26GST) glutathione transferases (*21*−*23*). In addition, in this paper, a kinetic unfolding study for the glutathione transferase supergene family will be reported for the first time. The kinetics of urea-induced unfolding of hGST A1-1 was performed using stopped-flow fluorescence. A general overview of the change in hGST A1-1 structure upon unfolding was provided by monitoring the changes in the optical properties of the intrinsic fluorophores (Tyr/Trp) and an extrinsic fluorophore (i.e., AEDANS covalently linked to Cys111). Unfolding kinetics monitored using tyrosine/tryptophan fluorescence is biphasic with a fast and a slow unfolding event, while unfolding kinetics using energy transfer to or direct excitation of Cys111−AEDANS is monophasic with properties similar to those observed for the slow unfolding event. The properties of the transition states for the fast and the slow unfolding events are closely related to native protein in terms of solvent exposure and hydrophobic interactions, and a sequential unfolding mechanism for hGST A1-1, which incorporates both events, is proposed.

MATERIALS AND METHODS

Materials. Ultrapure urea was purchased from ICN Biomedicals, Inc. IAEDANS, NATA, and *N*-acetyl-L-tyrosinamide were purchased from Sigma. All other reagents were of analytical grade. The plasmid, pKHA1, was a kind gift from B. Mannervik (*24*).

Expression and Purification of hGST A1-1. Recombinant human glutathione transferase A1-1 (hGST A1-1) was purified from pKHA1/JM 103 cells using *S*-hexylglutathione affinity chromatography (*24*). The protein was eluted from the affinity column using either 1 mM *S*-hexylglutathione or 50 mM glycine-NaOH, pH 10.0 (*19*). The homogeneity of the pure protein was assessed using SDS−PAGE (*25*) and SEC−HPLC. Protein concentration was estimated using a molar extinction coefficient of 38 200 M^{-1} cm^{-1} at 280 nm calculated by the method of Perkins (*26*).

Enzyme activity of native and alkylated hGST A1-1 was spectrophotometrically assessed at 340 nm in 0.1 M potassium phosphate buffer, pH 6.5, containing 1 mM 1-chloro-2,4-dinitrobenzene, 3% (v/v) ethanol, and 1 mM reduced glutathione (*27*).

Alkylation of hGST A1-1. hGST A1-1 was alkylated overnight with a 100-fold molar excess of IAEDANS at room temperature in 50 mM Tris-HCl, pH 7.5. Unreacted IAEDANS was separated from modified protein using gel filtration (Sephadex-G25). The stoichiometry of labeling was determined spectrophotometrically at 338 nm using an extinction coefficient of 6000 M^{-1} cm^{-1} for AEDANS (*28*). Enzyme activity, fluorescence spectroscopy, and SEC−HPLC were used to assess the modified enzyme, and its properties were found to be identical to those of native unmodified enzyme. This indicates that the chemical modification of Cys111 with the AEDANS group results in no gross conformational changes of the protein.

Equilibrium Studies. Unfolding and reversibility studies were performed at room temperature in 20 mM sodium phosphate, 1 mM EDTA, and 100 mM NaCl buffer, pH 6.5. Native and alkylated hGST A1-1 (0.8 μM) were unfolded in 0−8 M urea for at least 1 h. Reversibility of unfolding was initiated by a 10-fold dilution of enzyme (10 μM in 8 M urea) and assessed by enzyme activity and fluorescence spectroscopy.

Enzyme activity measurements of hGST A1-1, in the presence of denaturant, were assessed using the standard reaction assay described above. The final concentration of protein was 3 nM, and the residual denaturant had no effect on the activity of the enzyme. Linear progress curves exclude the influence of reactivation of denatured protein on the measurements obtained. All fluorescence measurements were made using a Hitachi model 850 fluorescence spectrofluorimeter. Tryptophan was selectively excited at 295 nm and emission monitored at 325 nm (folded) and 355 nm (unfolded). Steady-state fluorescence methods (i.e., tryptophan measurements, anisotropy decays, and ANS binding) and second-derivative analyses of UV spectra (tyrosine exposure) were performed as detailed for pGST P1−1 (*21, 22*). The analysis of the equilibrium unfolding curves and estimation of the conformational parameters used the linear extrapolation method of Pace (*29*) and are well-documented for glutathione transferases (*22, 23*).

Differential scanning calorimetric measurements were determined for 20 μM hGST A1-1 over a temperature range of 20−90 °C using the microcalorimeter DASM-4 (Mashipriborintork, Moscow). The change in heat capacity due to thermal unfolding was fitted to a two-state reaction scheme as detailed for sj26GST (*23*).

Kinetic Studies. Fluorescence detection of unfolding of hGST A1-1 was monitored using a stopped flow-mixing

device (SX-18 MV) from Applied Photophysics (U.K.). The excitation path length was 10 mm, and the emission path length was 2 mm. An excitation bandwidth of 2.32 nm was employed. The dead time of the instrument was measured using the reduction of 2,6-dichlorophenolindophenol (DCIP) by ascorbic acid at 524 nm (*30*). The mixing time of the instrument was 0.5 ms, and the dead time was calculated to be 1.5 ms; therefore no data within 2 ms was fitted. For unmodified hGST A1-1, fluorescence was measured by excitation of Tyr and Trp at 280 nm or Trp alone at 295 nm and the emission was monitored using a 320-nm cutoff filter. For AEDANS-modified protein, fluorescence was measured by direct excitation of AEDANS at 340 nm or energy transfer from Trp to AEDANS at 295 nm and emission was monitored using a 400-nm cutoff filter. The temperature in the stopped-flow cell was regulated within 0.1 °C of the required temperature using a thermostated water bath.

The kinetics of unfolding in the equilibrium transition, i.e., final urea concentrations between 3.5 and 4.5 M, was followed using manual mixing methods which have a dead time of 8−10 s. Fluorescence methods were made using a Hitachi model 850 fluorescence spectrofluorimeter with excitation at 280 nm and emission at 325 nm. The excitation and emission bandwidths were set to 5 nm each.

Kinetic Data Analysis. All kinetic data for unfolding were fitted using the Applied Photophysics software, version 4.24. The program utilizes the algorithm of Levenberg−Marquardt (*31*) for nonlinear least-squares fitting. Three to four kinetic runs were averaged per experiment and standard deviations calculated for at least three separate experiments. Kinetic analysis of the time-dependent change of fluorescence signal requires consideration of the final urea concentration with reference to the equilibrium transition.

For urea unfolding jumps ending at urea concentrations above the equilibrium transition zone (final urea concentrations greater than 6 M), the unfolding reactions of the fast and slow phases can be fitted using a single exponential. Each phase is fitted individually (by selecting a fitting range) to a single exponential:

$$F_t = F_i \exp(-t/\tau) + F_\infty \quad (1)$$

where F_t is the total fluorescence amplitude at time t, F_i is the fluorescence amplitude for phase i at time zero, τ is the time constant (the inverse of the apparent rate constant, k), and F_∞ is the fluorescence amplitude at infinite time.

For urea unfolding jumps ending with urea concentrations within the equilibrium transition zone (final urea concentrations 3.5−5.8 M), both unfolding and refolding reactions must be considered since in this region the model relaxes to equilibrium. Data in this region were analyzed using the relaxation expression described by Bernasconi (*32*).

For fluorescence measurements:

$$F_t = F_i(\exp(-t/\tau))/(1+q'F_i(1-\exp(-t/\tau))) + F_\infty \quad (2)$$

where F_t, F_i, F_∞, and τ have the same meaning as in eq 1. q' is the term which accounts for the quantum yields of the native and denatured states, the extinction coefficients of each species, and various instrumental parameters. In our study, as employed for the *Trp* aporepressor (*6*) and leucine zipper peptide (*33*), q' was used as a fitting parameter. In unfolding studies, q' has a theoretical limit of −0.5 (*32*). For these studies q' was typically −0.3. The term $q'F_i(1 - \exp(-t/\tau))$ in the denominator accounts for the contribution of the refolding reaction in the transition zone. This term approached zero under conditions that strongly favor the denatured state, and hence, it approximates to an equation equivalent to a single exponential (eq 1).

The deviations of the experimental data from the fitted function (i.e., the residuals) were used to judge the accuracy and quality of the fit.

Urea-Dependent Unfolding Experiments. In all experiments, unmodified/modified native protein (6 μM hGST A1-1 in 0 or 3 M urea in 20 mM sodium phosphate, 1 mM EDTA, and 100 mM NaCl buffer, pH 6.5) was diluted 6-fold (1:5 asymmetric mixing) with 4−10 M urea, at 25 °C. The final urea concentrations were between 3.5 and 8.9 M, and the final protein concentration was 1 μM. The urea dependence of the unfolding first-order rate constants (k_u) was fitted to eq 3 and enables the determination of the unfolding rate in the absence of denaturant (an estimate for the rate of dissociation/unfolding in vivo) and the change in solvent accessibility of the unfolded state (*34*):

$$\log k_u = \log k_u(H_2O) + m_u[\text{denaturant}] \quad (3)$$

where k_u is the apparent first-order rate constant for unfolding at different concentrations of denaturant, $k_u(H_2O)$ is the apparent unfolding rate in the absence of denaturant, and m_u is the change in solvent accessibility of the unfolded state.

Kinetic amplitudes for all phases (modified and unmodified protein) were normalized with respect to the fraction unfolded (f_u) measurements obtained in equilibrium studies.

Temperature-Dependent Unfolding Experiments. Temperature dependence of unfolding was performed at 10−40 °C by 6-fold dilution of 6 μM native protein with 10 M urea. The final urea concentration was 8.3 M. For modified protein, 6 μM native protein was diluted with 9.6 M urea to give a final concentration of 8 M. The temperature dependence of the apparent first-order rate constant for unmodified/modified protein was analyzed using the transition-state theory (Eyring plot) (*35*, *36*):

$$k_u = \kappa k_B T/h \exp(\Delta G^{\ddagger}/-RT) \quad (4)$$

where k_B is Boltzmann's constant, h is Planck's constant, T is the absolute temperature, R is the universal gas constant, and $\Delta G^{\ddagger}$ is the activation energy. The transmission coefficient (κ) is assumed to equal 1. The temperature dependence of the apparent first-order rate constant (k_u) reflects the temperature dependence of the free energy of activation $\Delta G^{\ddagger}$ (*35*):

$$\Delta G^{\ddagger}(T_o) = \Delta H^{\ddagger}(T_o) - T\Delta S^{\ddagger}(T_o)$$

$$= \Delta H^{\ddagger}(T_o) + \Delta C_p{}^{\ddagger}(T - T_o) - T[\Delta S^{\ddagger}(T_o) + \Delta C_p{}^{\ddagger} \ln(T/T_o)] \quad (5)$$

where T is the absolute temperature, T_o is the standard temperature (298 K), $\Delta S^{\ddagger}(T_o)$ is the activation entropy at T_o, $\Delta H^{\ddagger}(T_o)$ is the activation enthalpy at T_o, and $\Delta C_p{}^{\ddagger}$ is the heat capacity difference between the native and transition state.

Substitution of eq 5 into (4) yields:

$$\ln(k_u h/k_B T) = [\Delta S^{\ddagger}(T_o)/R - \Delta H^{\ddagger}(T_o)/RT - \Delta C_p^{\ddagger}(T - T_o)/RT + \Delta C_p^{\ddagger}/R \ln(T/T_o)] \quad (6)$$

which enables a plot of $\ln(k_u h/k_B T)$ versus $1/T$ to be fitted and the thermodynamic parameters of the unfolding kinetics to be calculated. Data were fitted using linear least-squares iteration by the program Sigma Plot (version 5.0) (Jandel Corp.).

RESULTS

Fluorescence Properties of hGST A1-1. Human class α glutathione transferase contains one tryptophan residue (Trp20) per subunit, located at the interdomain interface in α helix 1 of domain I (Figure 1) (*18*). The indole side chain of Trp20 protrudes from domain I into domain II and has nonspecific hydrophobic interactions with the side chains of Ile158, Glu162, and Tyr165 (all in α helix 6) and Val194 and Phe197 (in α helix 8). The side chain of Trp20 is inaccessible to solvent (SASA is 4 Å^2) and can be used as a probe for the dissociation of the two domains (*20*). Fluorescence spectra of native and unfolded hGST A1-1 indicate that the native protein has a greater intrinsic fluorescence than the denatured protein; therefore complete unfolding results in a decrease in fluorescence intensity.

In the crystal structure, hGST A1-1 has 10 tyrosines with an average percentage solvent accessibility of 19.1 Å^2; three are located in domain I, two in the linker region, and five in domain II. Excitation at 280 nm yields an emission maximum (325 nm) which is identical to that for direct excitation of tryptophan (at 295 nm), and the emission spectrum indicates a substantial amount of energy transfer from the tyrosines (globally distributed) to the tryptophan. Therefore, Trp20 is a local reporter of events occurring at the interdomain interface.

The single cysteine in hGST A1-1, Cys111, is located in the turn between the α helices 4 and 5 of domain II. Its sulfydryl side chain is exposed to solvent (SASA is 21 Å^2) and points into the amphipathic V-shaped cavity between the two subunits (L-site) (Figure 1). The thiol group of Cys111 in subunit 1 is 23 Å from the ϵ-nitrogen of the indole group Trp20 in the same subunit and 34 Å from the ϵ-nitrogen of the indole group in subunit 2. The location of Cys111 enables it, by means of AEDANS modification, to be employed to monitor changes occurring at the cleft between the two subunits.

The fluorescent properties of tyrosine and tryptophan (excitation at 280 nm) and tryptophan alone (excitation at 295 nm), in addition to chemically modified Cys111 (Cys111−AEDANS) (excitation at 295 or 340 nm), were used to probe the urea-induced conformational changes of hGST A1-1.

Equilibrium Unfolding of hGST A1-1 Is Two-State. The reversibility of equilibrium unfolding was assessed by a 10-fold dilution of denatured hGST A1-1 and monitored using fluorescence spectroscopy and enzyme activity. Refolded hGST A1-1 has an emission maximum (325 nm) and intensity identical to that of native protein. In addition, the recovery of enzyme activity was 95−98%. Similarly, refolded Cys111−AEDANS hGST A1-1 was structurally (100%) and functionally (90%) similar to native protein.

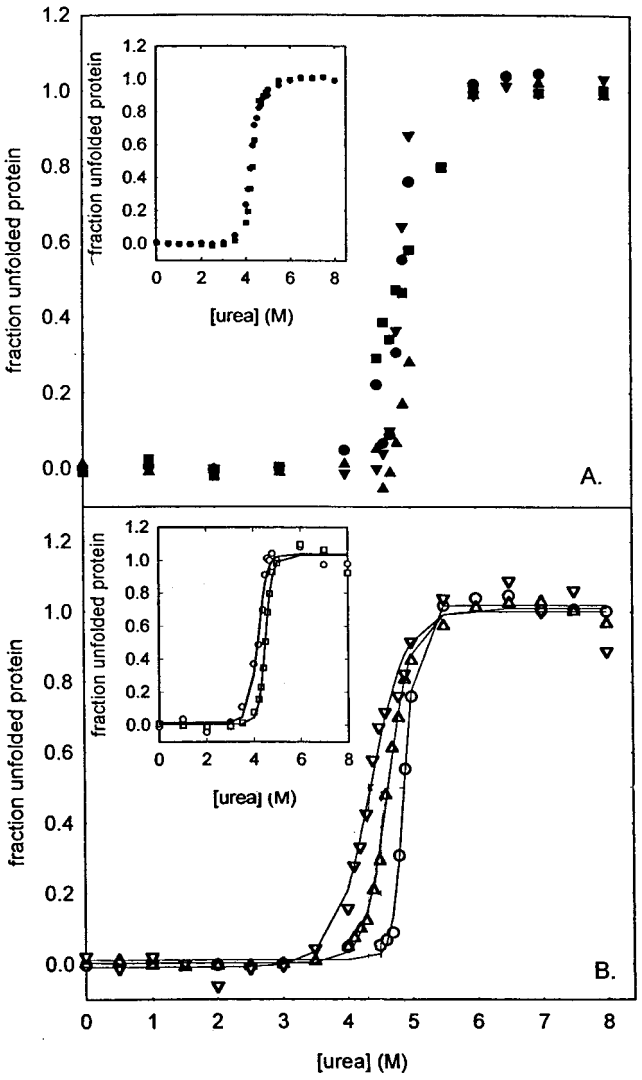

FIGURE 2: (A) Urea-induced equilibrium unfolding curves for 5 μM hGST A1-1 monitored by Trp20 fluorescence (●), anisotropy decays (■), binding of ANS (▲), and extent of tyrosine exposure (▼). Inset: equilibrium unfolding transition for unmodified hGST A1-1 (■) and AEDANS-alkylated Cys111 hGST A1-1 (●). Tryptophan was selectively excited at 295 nm and emission measured at 325 and 355 nm. Each experiment was performed using 0.8 μM hGST A1-1 in 0.1 M NaCl, pH 6.5, 25 °C. (B) Equilibrium unfolding transition curves for enzyme activity (○) and fluorescence (□) measurements.

The equilibrium unfolding reaction of hGST A1-1, induced by urea, shows a single sigmoidal transition indicative of a highly cooperative system involving native dimer and two unfolded monomers (Figure 2). The two-state (folded dimer/unfolded monomer) transition was supported by coincident unfolding transition curves using various structural probes (i.e., tryptophan fluorescence, tyrosine exposure, anisotropy decays, and 8-anilino-1-naphthalenesulfonate (ANS) binding) (Figure 2a) and protein concentration dependence of the midpoint of the unfolding transition (i.e., increased stability with increasing protein concentration) (Figure 2b). The values for the free energy change in the absence of denaturant, normalized to 1 M protein, for these curves are in close agreement (0.1 μM hGST A1-1, $\Delta G(H_2O) = 25.98$

(±3.23) kcal mol^{-1}; 1 μM hGST A1-1, $\Delta G(H_2O)$ = 27.59 (±3.80) kcal mol^{-1} and 5 μM hGST A1-1, $\Delta G(H_2O)$ = 26.68 (±4.09) kcal mol^{-1}) which validates the two-state model. The experimentally determined parameters are in agreement with those predicted by Neet and Timm (*37*) and Myers et al. (*38*). The individual curves obtained for hGST A1-1 and Cys111−AEDANS hGST A1-1 are coincident within experimental error (Figure 2A, inset).

The sigmoidal unfolding transition obtained using enzyme activity (as a functional probe) was noncoincident with those obtained using structural probes (Figure 2B, inset). The unfolding transition for 1 μM hGST A1-1 has a midpoint at 4.1 M urea for enzyme activity measurements and at 4.5 M urea for fluorescence measurements.

In addition, the two-state assumption is supported by the correlation between the calorimetric enthalpy (ΔH_{cal} = 398.9 kcal/mol) and the van't Hoff enthalpy ($\Delta H_{v,H}$ = 358.3 kcal/mol) (see ref *23* for an example of a thermogram). For the two-state assumption (i.e., no intermediates), $r = \Delta H_{cal}/\Delta H_{v,H}$ approximates to unity (*39*). For hGST A1-1, r = 0.90.

Unfolding Kinetics of hGST A1-1. Figure 3 illustrates the unfolding kinetic traces for unmodified hGST A1-1 (Figure 3A and inset) and for AEDANS-modified hGST A1-1 (Figure 3B). Unfolding kinetic traces for unmodified hGST A1-1 monitored using tryptophan fluorescence does not show a simple monophasic change (Figure 3A and inset). Two kinetic phases were observed for final urea concentrations between 3.5 and 8.9 M and over a 10−40 °C temperature range. The unfolding phases will be referred to as fast and slow unfolding events. Generally, the fast phase occurs in the millisecond time range and the slow phase in the second to minutes time range. The fluorescence signal for the fast phase increases while the fluorescence signal for the slow phase decreases relative to the signal for native folded protein. For the final urea unfolding condition of 8.3 M (Figure 3), the rate constants for the fast phase (inset of panel A) and slow phase (panel A) are 48.70 (±3.26) and 0.24 (±0.03) s^{-1}, respectively. The initial and final amplitudes are as predicted by equilibrium experiments indicating that no burst phase occurs within the dead time.

Various control experiments established that both phases were real unfolding events and that they were not the results of mixing artifacts. Identical "unfolding" experiments were performed using 2 μM *N*-acetyl-L-tryptophanamide (NATA) and 20 μM *N*-acetyl-L-tyrosinamide instead of hGST A1-1. "Unfolding" monitored by excitation at 280 nm and final urea conditions of 8.3 M yielded a horizontal signal response. In addition, if the fast phase were a mixing artifact or the result of aggregation, it would be observed at any wavelength as a consequence of a change in refractive index. Absorbance at 340 nm, used to monitor aggregation in this study, shows a horizontal signal response with no change in amplitude. Finally, all control runs (buffer only, buffer/urea, and buffer/protein) showed no signal change. The effect of residual *S*-hexylglutathione on the unfolding kinetics can be excluded since protein prepared in the absence of ligand (*19*) displayed identical biphasic behavior.

Unfolding kinetics of Cys111−AEDANS hGST A1-1 monitored by energy transfer from Trp20 to Cys111−AEDANS (Figure 3B) and the direct excitation of Cys111−AEDANS (results not shown) showed a monophasic change. The single phase accounts for all of the amplitude predicted by equilibrium experiments. This single unfolding phase displayed similar urea-dependence properties as observed for the slow unfolding phase monitored using tyrosine/tryptophan fluorescence. The absence of a detectable lag phase, for the identical time period in which the fast unfolding phase monitored using tryptophan fluorescence was observed, is depicted in the inset of Figure 3B. For modified hGST A1-

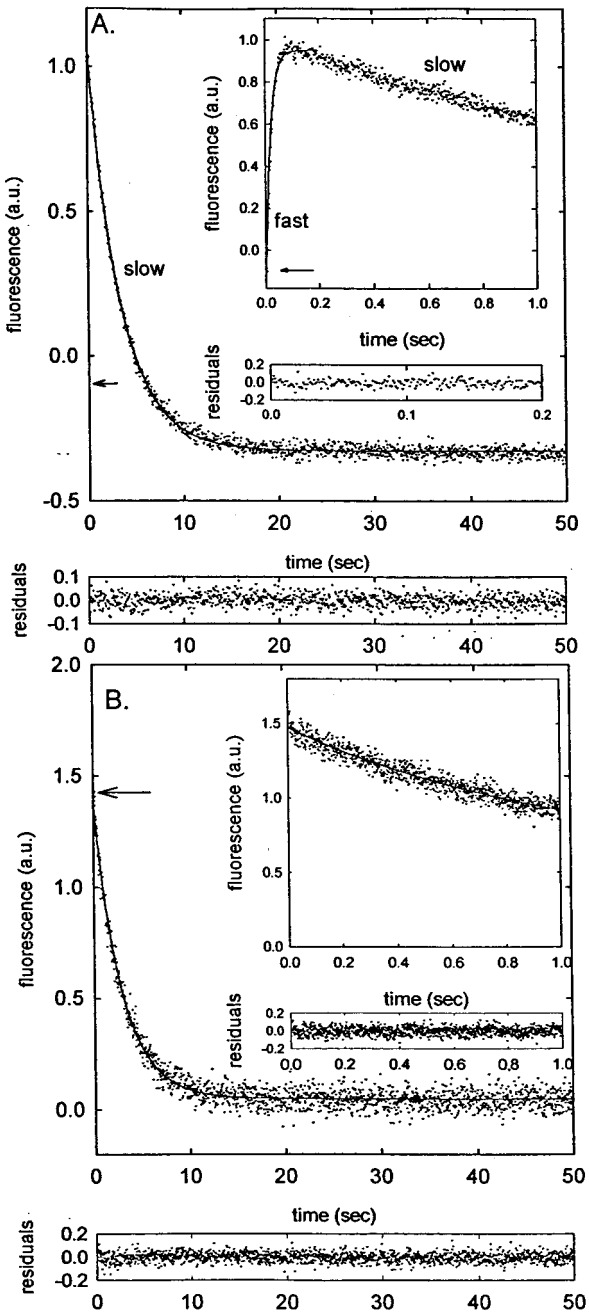

FIGURE 3: Unfolding kinetics. Final urea concentration of 8.3 M, pH 6.5, 25 °C. The change in fluorescence of unmodified 1 μM hGST A1-1 was monitored by excitation at 280 nm and emission above 320 nm. The fast phase, part of the slow phase (inset), and the slow phase alone (A) are shown. Panel B shows the fluorescence change of 0.8 μM Cys111−AEDANS hGST A1-1 monitored by excitation at 295 nm and emission above 400 nm and the absence of a lag phase (inset of panel B). The arrows indicate the fluorescence signal for native folded protein. The unfolding kinetic traces were fitted with a single-exponential function. The lower panels show the residuals (the difference between the data and the fitted function) for the corresponding kinetic traces.

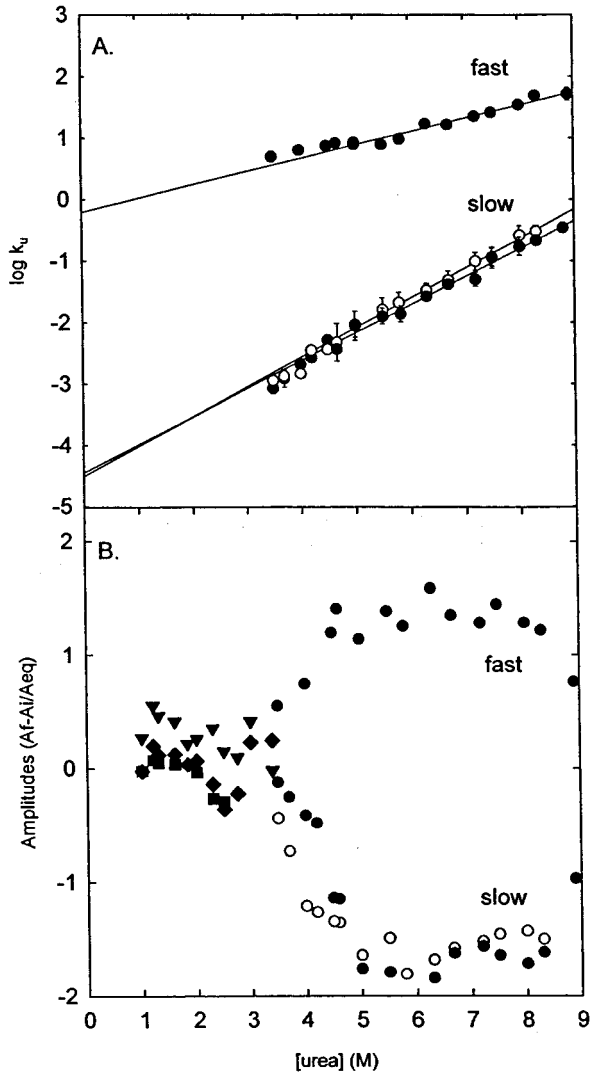

FIGURE 4: (A) Urea dependence of the unfolding rate constants for 1 μM unmodified hGST A1-1 (●) and 0.8 μM Cys111−AEDANS hGST A1-1 (○). The solid lines are the curve fits using eq 3. Unfolding experiments were performed at 25 °C, 0.1 M NaCl, pH 6.5. Data were fitted to eq 2 for urea concentrations between 4.5 and 5.8 M urea and to eq 1 for final urea concentrations greater than 5.8 M. The error bars are as indicated or are comparable to the size of the symbol. (B) Urea dependence of the amplitudes for unfolding (●) and refolding (▼, ◆, ■) of unmodified hGST A1-1. The urea dependence of the amplitudes for unfolding for Cys111−AEDANS hGST A1-1 is also indicated (○). The amplitudes were normalized with respect to the fraction unfolded measurements obtained in equilibrium studies.

1, the rate constant for unfolding at 8.3 M urea was 0.29 ($\pm$0.04) s^{-1}.

In control experiments, the time constants for the fast and slow unfolding phases were independent of protein concentration over a 0.5−5 μM range. Therefore these reactions are unimolecular and reflect unfolding events and not higher order aggregation.

Urea Dependence of the Unfolding Rate. The rate of unfolding of unmodified/AEDANS-modified protein increases as conditions favor the unfolded state. For unmodified protein, the urea dependence of the unfolding data (Figure 4A) for both fast and slow phases fits well to a linear regression ($r = 0.998$ and 0.996, respectively) and similarly for the single phase observed for Cys111−AEDANS hGST A1-1 ($r = 0.991$). The linear dependence of the unfolding rate on denaturant suggests that no changes occur in the rate-limiting step and that the unfolded species formed differ from the native state of hGST A1-1 with respect to solvent exposure. Refolding studies with hGST A1-1 are consistent with a rate-limiting step which is urea and protein concentration-dependent (Wallace and Dirr, unpublished results) suggesting that the nature of the rate-limiting step for folding and unfolding involves the transition between two unfolded monomers and one dimer. The urea dependence of unfolding/refolding has a minimum at approximately 4.6 M urea, consistent with the midpoint of the equilibrium unfolding curve for 1 μM protein (at approximately 4.3 M urea), demonstrating the reversibility of this unfolding/folding system.

For unmodified hGST A1-1, the apparent rate constant for unfolding of the fast phase is less urea sensitive than the slow phase (Figure 4A). The slopes (m_u) of the fast and slow phases are 119.5 and 270 cal/mol/M of urea, respectively. The fast phase therefore results in an unfolded species that is more closely related to the native state of hGST A1-1 in terms of solvent exposure. For modified hGST A1-1, the single unfolding phase has a slope (m_u) of 286.2 cal/mol/M urea. The similar urea dependence for unmodified and modified hGST A1-1 supports the suggestion that this phase is similar to the slow phase for unmodified protein.

The ratio of m_u/m (where m_u is RT log k_u/[urea] (Figure 4A) divided by the m value obtained for 1 μM hGST A1-1 in equilibrium studies (4.22 $\pm$ 0.72 kcal/mol/M urea)) is an indication of the increase in solvent exposure of the transition state relative to the native state, normalized by the increase in solvent exposure between the native and denatured state (*34*). For Cys111−AEDANS hGST A1-1, the ratio of m_u/m is 0.068, which is suggestive of a transition state for the single unfolding phase of modified protein with a solvent accessibility closely related to that of the native state, i.e., 6.8% of the buried hydrophobic surface in the native state is exposed at the transition state. The slow unfolding phase for unmodified protein has a m_u/m ratio of 0.064, which is comparable with that for AEDANS-modified protein. The fast unfolding phase for unmodified protein has a m_u/m ratio of 0.028 indicating that this transition state relates more closely to the accessible surface area of the native protein. A ratio that approximates to unity would be indicative of a transition state that is as solvent-exposed as the denatured state (*40*).

For unmodified hGST A1-1, the unfolding rates in the absence of denaturant (k_u (H_2O)) are 0.61 and 2.92 $\times$ 10^{-5} s^{-1} for the fast and slow phases, respectively (as obtained from the zero urea intercepts in Figure 4A). These results correspond to time constants of 1.6 s and 9.5 h for the fast and slow phases, respectively. Cys111−AEDANS hGST A1-1 has a similar zero urea intercept (3.07 $\times$ 10^{-5} s^{-1}) and time constant for unfolding in the absence of denaturant (9.0 h) as the slow unfolding phase for unmodified protein.

Urea Dependence of the Unfolding Amplitudes. The urea dependence of the amplitudes for the fast and slow unfolding phases for unmodified protein and for the single unfolding phase for modified protein is depicted in Figure 4B. Both the fast and slow phases occur simultaneously from 3.5 M urea. The relative percentages of the two species increased from 3.5 to 5 M urea and then became independent of the urea concentration when the final urea concentration exceeded 5 M urea. The inverse amplitudes are the result of

the different fluorescence properties of each phase. The occurrence of both phases from time zero suggests that the slow phase overlaps the fast phase, and it is therefore quite likely that the parameters obtained for the fast unfolding phase are underestimated. The amplitudes for the single unfolding phase for AEDANS-modified protein display similar characteristics to those for the slow unfolding of unmodified protein. The amplitudes for the three refolding phases were included to illustrate the consistency of the unfolding/refolding transition for hGST A1-1.

The biphasic unfolding kinetics that were observed for unmodified hGST A1-1 suggests that more than the two species (folded dimer/unfolded monomer) predicted by equilibrium studies must be present along the unfolding pathway (*41*). The unfolding amplitudes and rates for hGST A1-1 using the same final urea concentration (8 M) but varying the initial urea concentration (up to 3 M urea, where the protein is in the folded form) were measured. The change in the initial conditions had no effect on the amplitudes and rates on the fast and slow phases (results not shown) negating the presence of different native forms in the equilibrium pretransition zone and confirming that the fast phase is an unfolding event.

Temperature Dependence of the Unfolding Rates. The apparent unfolding rates of the fast and slow phases of unmodified hGST A1-1 were further characterized from 10 to 40 °C at a final urea concentration of 8.3 M. The temperature-dependence for the single unfolding phase for AEDANS-modified protein was characterized at a final urea concentration of 8 M. For unmodified hGST A1-1, both phases are temperature dependent with the apparent unfolding rate and amplitude of the fast phase increasing to such an extent at 40 °C that the fast phase occurred within the dead time. The rate constant for unfolding was related to the Gibbs free energy ($\Delta G^{\ddagger}$) of activation using the transition-state theory (*36*). For both phases, the plot of $\ln(k_u h/k_B T)$ versus $1/T$ (Figure 5A) is almost linear. Both phases fit equally well to eq 6 and to a linear fit (see residuals in Figure 5B).

The best fit for eq 6 to the fast unfolding phase of unmodified protein gives the following thermodynamic parameters: $\Delta C_p^{\ddagger}$ of 253.3 cal^{-1} mol^{-1} K^{-1}, $\Delta H^{\ddagger}$(298 K) of 20.45 kcal mol^{-1}, $\Delta S^{\ddagger}$(298 K) of 17.45 cal^{-1} mol^{-1} K^{-1}. Fitting the data of the slow unfolding phase of unmodified protein to eq 6 gives: $\Delta C_p^{\ddagger}$ of 475.0 cal^{-1} mol^{-1} K^{-1}, $\Delta H^{\ddagger}$(298 K) of 18.90 kcal mol^{-1}, $\Delta S^{\ddagger}$(298 K) of 2.28 cal^{-1} mol^{-1} K^{-1}. For the single unfolding phase of Cys111-AEDANS hGST A1-1, the temperature dependence of the apparent unfolding rate constant shows distinct curvature when fitted to eq 6 and the residuals indicate that the unfolding rate is best-fitted to this. equation than to a linear function. The curvature occurs at the temperature extremes and may indicate systematic deviation of the data rather than a large heat capacity ($\Delta C_p^{\ddagger}$) change as the protein unfolds. The best fit for eq 6 to the single phase for modified protein gives: $\Delta C_p^{\ddagger}$ of 987.0 cal^{-1} mol^{-1} K^{-1}, $\Delta H^{\ddagger}$(298 K) of 18.46 kcal mol^{-1}, $\Delta S^{\ddagger}$(298 K) of 0.878 cal^{-1} mol^{-1} K^{-1}. The errors from the fit to eq 6 (not shown) are large since the curvature is marginal in the experimentally accessible temperature range (*36*).

The linearity of the temperature-dependent data, monitored using tyrosine/tryptophan fluorescence, is consistent with a small heat capacity change ($\Delta C_p^{\ddagger} = 0$) between the native state and the transition states. Changes in the heat capacity (ΔC_{pN-U}) and *m* values for unfolding can be estimated by relating the surface area exposed to the size of the protein (*38*). For hGST A1-1 the heat capacity change for complete unfolding is estimated to be 7.3 kcal^{-1} mol^{-1} K^{-1}. To determine relative heat capacity changes, this value is used instead of the value obtained calorimetrically (DSC) since the glutathione transferase system for thermal unfolding is complicated by irreversibility and aggregation (*23*). The extent of buried surface area for each transition state ($\Delta C_p^{\ddagger}/\Delta C_{pN-U}$) is 3.4% and 6.5% for the fast and slow unfolding phases of unmodified protein, respectively, and 13.5% for the single unfolding phase of Cys111−AEDANS hGST A1-1. The compactness of the unfolding transition states is therefore in agreement with the urea and temperature data shown above.

The activation energy (calculated using $\Delta H^{\ddagger} = E_A - RT$ (*35*) or obtained from a linear Arrhenius plot) is 21.04 (±1.89) and 19.49 (±1.51) kcal mol^{-1} for the fast and slow unfolding phases of unmodified protein, respectively. Similarly, for the single unfolding phase for Cys111−AEDANS hGST A1-1, the activation energy is 19.05 (±2.15) kcal

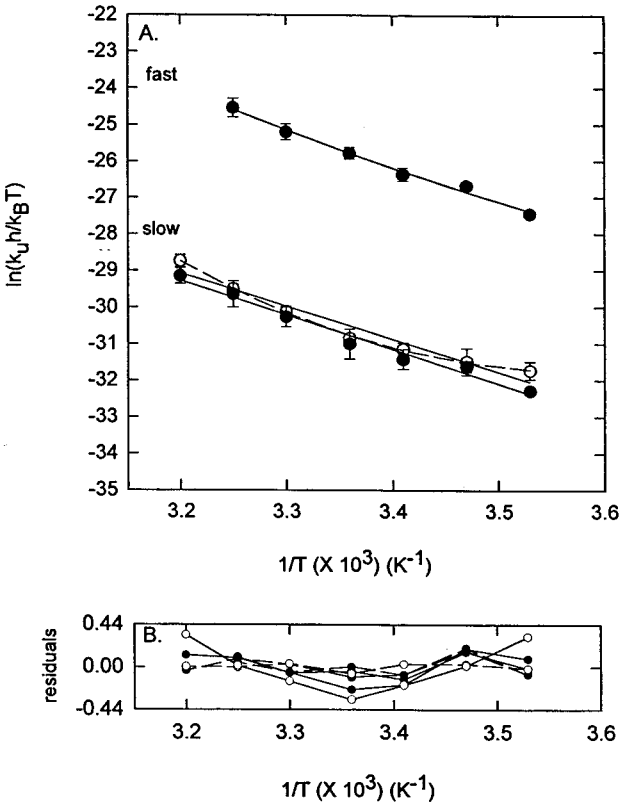

FIGURE 5: Eyring plots for the temperature dependence of the unfolding rate constant for 1 μM unmodified hGST A1-1 (●) and 0.8 μM Cys111−AEDANS hGST A1-1 (○). Unfolding experiments were performed at 8.3 M urea, 0.1 M NaCl, pH 6.5, for unmodified hGST A1-1 and at 8 M urea, 0.1 M NaCl, pH 6.5, for Cys111−AEDANS hGST A1-1. The error bars are as indicated or are comparable to the size of the symbol. The plots for unmodified hGST A1-1 (●) fit equally well to a linear function (solid lines) and eq 6 (dashed line). The plot for Cys111−AEDANS hGST A1-1 (○) is best-fitted to eq 6 (dashed line). The residuals for fitting to a linear function (solid lines, (●) unmodified hGST A1-1, (○) Cys111−AEDANS hGST A1-1) and eq 6 (dashed lines, (●) unmodified hGST A1-1, (○) Cys111−AEDANS hGST A1-1) are indicated in panel B.

mol^{-1}. The high activation energy for unfolding is indicative of the large number of forces required to maintain the native structure (*4*). For the slow phase, the time range and the activation energy could be indicative of cis X−Pro peptide bond isomerization (*42*). However, the urea dependence of the slow phase excludes the possibility of such an isomerization.

The apparent activation Gibbs free energies in the absence of denaturant ($\Delta G^{\ddagger}(H_2O)$) calculated for the fast and slow unfolding phases according to eq 4 are 17.74 and 23.59 kcal mol^{-1}, respectively. Therefore, the slow unfolding phase represents the transition state for the overall unfolding pathway.

DISCUSSION

Equilibrium Unfolding of hGST A1-1. Equilibrium unfolding of hGST A1-1 is consistent with a two-state transition between native dimer (N_2) and unfolded monomer (U) (i.e., $N_2 \rightleftharpoons 2U$). This simple dynamic equilibrium is consistent with an "all-or-none" process for unfolding of a homogeneous population of native protein and is well-documented for a large number of proteins (*43*) including the glutathione transferases (*21*−*23*). The noncoincidence of the unfolding transition for enzyme activity and Trp fluorescence does not exclude an equilibrium two-state behavior (*44*, *45*). This phenomenon may be the consequence of the highly flexible α helix 9 found in the C-terminal of the GST A1-1 polypeptide chain (*19*). It is feasible that the conformational flexibility of this helix would render it more susceptible to urea than the rest of the protein molecule and that destabilization of this structural motif would impact on the hydrophobic substrate binding site and the catalytic function.

The absence of a folded monomeric or dimeric intermediate for proteins such as the Arc repressor (*46*), the *Trp* aporepressor (*6*), and the cytosolic glutathione transferases suggests that each monomer cannot be separated into distinct folding units. All subunits of the glutathione transferases have been described, albeit subjectively by eye, as comprising of two domains. Domains I and II of each subunit were identified by visual inspection of the crystal structure of the porcine class π glutathione transferase (pGST P1-1) (*47*). An algorithm described by Siddiqui and Barton (*48*) was designed to accurately identify domains and identified each subunit of the glutathione transferase as being comprised of only one domain. The reason for this may be attributed to the large number of interdomain interactions.

For hGST A1-1, as for all cytosolic glutathione transferases studied thus far, the free energy of stabilization of the native three-dimensional state is high (approximately 25 kcal/mol). This implies that the quaternary structure of all cytosolic glutathione transferases is necessary for stabilization of the native state. All cytosolic glutathione transferases have distinct quaternary structures which are composed of identical or nonidentical subunits with interactions at the subunit interface formed primarily between domain I (α helix 2) of one subunit and domain II (α helices 3 and 4) of the adjacent subunit.

Unfolding Kinetics of hGST A1-1. The unfolding kinetics of unmodified hGST A1-1 is biphasic with a fast unfolding event and a slower main unfolding event. The increase in intensity for the fast phase indicates that Trp20 is transiently exposed to solvent and is postulated to represent the partial dissociation of domains I and II of each subunit. Complexities in kinetic unfolding reactions are rare since the transition state for unfolding is structurally related to the native state. For many monomeric proteins (*3*) and for the few oligomeric proteins studied (*5*, *6*, *8*), unfolding kinetics is monophasic, consistent with an "all-or-none" unfolding mechanism for a homogeneous population of protein.

Complex unfolding reactions have been observed for some proteins and originate from either multiple states of the native protein or from kinetic coupling between peptide bond isomerization and the actual folding reaction (*2*), for example, monomeric RNase (*10*, *49*) and monomeric dihydrofolate reductase (DHFR) (*50*). Proteins that unfold via a structural intermediate often display nonlinear denaturant dependence of the rate of unfolding (referred to as a "rollover") at high denaturant concentrations. The "rollover" is indicative of a change in the rate-limiting step and has been observed for the P22 Arc repressor (*51*), staphylococcal nuclease (*52*), and *Rhodobacter capsulatus* cytochrome c_2 (*53*). The absence of a "rollover" for hGST A1-1 suggests that there is no change in the rate-limiting step, and therefore the fast unfolding event represents a partial dissociation of the two domains rather than the formation of a structured intermediate.

A sequential unfolding pathway, based on structural and experimental evidence, describes the unfolding properties of hGST A1-1:

$$N_2 \rightarrow N_2^* \rightarrow 2U_A$$

where N_2 represents the folded dimeric state, N_2^* represents a nativelike dimer or dimeric intermediate, and U_A is an unfolded monomeric state of hGST A1-1. The inclusion of an additional isomerization reaction between different unfolded states of hGST A1-1 is supported by crystallographic evidence (*18*). The reaction $2U_A \rightleftharpoons 2U_B$ would represent the cis/trans isomerization of X−Pro peptide bonds. Cis/trans proline isomerization was not observed since the conditions used were insensitive to structures that vary only in their bond orientations.

The pathway proposed incorporates the two events observed using Tyr/Trp and only Trp fluorescence as well as the single event monitored by energy transfer to or direct excitation of Cys111, which was covalently labeled with the fluorescent AEDANS group. For the pathway monitored using Tyr/Trp fluorescence, the fast unfolding event can be described by the $N_2 \rightarrow N_2^*$ reaction. This event is proposed to represent the partial dissociation of the two structurally distinct domains, at the domain interface, near the Trp20. The dissociation results in a nativelike dimeric state or dimeric intermediate that resembles the folded state in terms of solvent exposure and hydrophobic interactions. The fast unfolding event is followed by a slower unfolding event ($N_2^* \rightarrow 2U_A$) which represents complete dissociation and unfolding of the nativelike dimer into two unfolded monomers. This event is also represented by the single phase observed using AEDANS-labeled Cys111 hGST A1-1. The two-state (dimer/monomer) equilibrium unfolding transition excludes the presence of a stable folded monomeric state along the unfolding pathway. The slow unfolding event observed using Tyr/Trp fluorescence and the single event observed

using AEDANS-labeled hGST A1-1 have similar urea and temperature properties suggesting that their transition states occupy similar positions on the reaction coordinate profile based on solvent accessibility.

The sequential unfolding pathway proposed at this stage represents the most satisfactory and simplest model necessary to describe the unfolding properties of hGST A1-1. Further characterization of the fast and slow unfolding events, using structural probes and mutational studies, will enable a better understanding of the structural basis for the unfolding mechanism of hGST A1-1.

REFERENCES

1. Anfinsen, C. B. (1973) *Science (Washington, DC) 181*, 223−230.
2. Kiefhaber, T. (1995) In *Methods in Molecular Biology, Vol. 40: Protein Stability and Folding: Theory and Practice* (Shirley, B. A., Ed.) pp 313−341, Humana Press Inc., Totowa, NJ.
3. Kim, P. S., and Baldwin, R. L. (1990) *Annu. Rev. Biochem. 59*, 631−660.
4. Matthews, C. R. (1993) *Annu. Rev. Biochem. 62*, 653−683.
5. Milla, M. E., and Sauer, R. T. (1994) *Biochemistry 33*, 1125−1133.
6. Gittelman, M. S., and Matthews, C. R. (1990) *Biochemistry 29*, 7011−7020.
7. Mann, C. J., and Matthews, C. R. (1993) *Biochemistry 32*, 5282−5290.
8. Liang, H., and Terwilliger, T. C. (1991) *Biochemistry 30*, 2772−2782.
9. Blond, S., and Goldberg, M. E. (1985) *J. Mol. Biol. 182*, 587−606.
10. Houry, W. A., and Scheraga, H. A. (1996) *Biochemistry 35*, 11719−11733.
11. Mannervik, B., Alin, P., Guthenberg, C., Jenssen, H., Tahir, M. K., Warholm, M., and Jornvall, H. (1985) *Proc. Natl. Acad. Sci. U.S.A. 82*, 7202−7206.
12. Ji, X., von Rosenvinge, E. C. M., Johnson, W. W., Tomarev, S. I., Piatigorsky, J., Armstrong, R. N., and Gilliand, G. J. (1995) *Biochemistry 34*, 5317−5328.
13. Meyer, D. J., Coles, B., Pemble, S. E., Gilmore, K. S., Fraser, G. M., and Ketterer, B. (1991) *Biochem. J. 274*, 409−414.
14. Pemble, S. E., Wardle, A. F., and Taylor, J. B. (1996) *Biochem. J. 319*, 749−754.
15. Dirr, H. W., Reinemer, P., and Huber, R. (1994) *Eur. J. Biochem. 220*, 645−661.
16. Wilce, M. C. J., and Parker, M. W. (1994) *Biochim. Biophys. Acta 1205*, 1−18.
17. Armstrong, R. N. (1994) *Adv. Enzymol. Relat. Areas Mol. Biol. 69*, 1−44.
18. Sinning, I., Kelywegt, G. J., Cowan, S. W., Reinemer, P., Dirr, H. W., Huber, R., Gilliand, G. L., Armstrong, R. N., Ji, X., Board, P. G., Olin, B., Mannervik, B., and Jones, T. A. (1993) *J. Mol. Biol. 232*, 192−212.
19. Cameron, A. D., Sinning, I., L'Hermite, G., Olin, B., Board, P. G., Mannervik, B., and Jones, T. A. (1995) *Structure 3*, 717−727.
20. Atkins, W. M., Dietze, E. C., and Ibarra, C. (1997) *Protein Sci. 6*, 873−881.
21. Dirr, H. W., and Reinemer, P. (1991) *Biochem. Biophys. Res. Commun. 180* (1), 294−300.
22. Erhardt, J., and Dirr, H. W. (1995) *Eur. J. Biochem. 230*, 614−620.
23. Kaplan, W., Hüsler, P., Klump, H., Erhardt, J., Sluis-Cremer, N., and Dirr, H. W. (1997) *Protein Sci. 6*, 399−306.
24. Stenberg, G., Bjornestedt, R., and Mannervik, B. (1992) *Protein Exp. Purif. 3*, 80−84.
25. Laemmli, U. K. (1970) *Nature (London) 227*, 680−685.
26. Perkins, S. J. (1986) *Eur. J. Biochem. 157*, 169−180.
27. Habig, W. H., and Jakoby, W. B. (1981) *Methods Enzymol. 77*, 398−405.
28. Hudson, E. N., and Weber, G. (1973) *Biochemistry 12*, 4154−4161.
29. Pace, C. N., Shirley, B. A., and Thomson, J. A. (1989) In *Protein Structure*: A Practical Approach, 2nd ed. (Creighton, T. E., Ed.) pp 311−330, IRL Press, Oxford University Press, Oxford.
30. Tonomura, B., Nakatani, H., Ohnishi, M., Yamaguchi-Ito, J., and Hiromi, K. (1978) *Anal. Biochem. 84*, 370−383.
31. Marquardt, N. (1963) *J. Soc. Ind. Appl. Math. 11*, 431−441.
32. Bernasconi, C. F. (1976) *Relaxation Kinetics*, pp 76−97, Academic Press, New York.
33. Wendt, H., Leder, I., Härma, H., Jelesarov, I., Baici, A., and Bosshard, H.R. (1997) *Biochemistry 36*, 204−213.
34. Tanford, C. (1970) *Adv. Protein Chem. 24*, 1−95.
35. Oliveberg, M., Tan, Y.-J., and Fersht, A. R. (1995) *Proc. Natl. Acad. Sci. U.S.A. 92*, 8926−8929.
36. Tan, Y.-T., Oliveberg, M., and Fersht, A. R. (1996) *J. Mol. Biol. 264*, 377−389.
37. Neet, K. E., and Timm, D. E. (1994) *Protein Sci. 3*, 2167−2174.
38. Myers, J. K., Pace, C. N., and Scholz, J. M. (1995) *Protein Sci. 4*, 2138−2148.
39. Marky, L. A., and Breslauer, K. J. (1987) *Biopolymers 26*, 1601−1620.
40. Doyle, D. F., Waldner, J. C., Parkh, S., Alcazar-Roman, L., and Pielak, G. J. (1996*) Biochemistry 35*, 7403−7411.
41. Hagerman, P. J., and Baldwin, R. L. (1976) *Biochemistry 15*, 1462−1473.
42. Nall, B. T., Garel, J., and Baldwin, R. L. (1978) *J. Mol. Biol. 118*, 317−330.
43. Schmid, F. X. (1992) In *Protein Folding* (Creighton, T., Ed.) pp 197−241, W. H. Freeman and Co., New York.
44. Dill, K. A., and Shortle, D. (1991) *Annu. Rev. Biochem. 60*, 795−825.
45. Chan, H. S., Bromberg, S., and Dill, K. A. (1995) *Philos. Trans. R. Soc. London B 348*, 61−70.
46. Bowie, J. U., and Sauer, R. T. (1989) *Biochemistry 28*, 7139−7143.
47. Reinemer, P., Dirr, H. W., Ladenstein, R., Schaffer, J., Gallay, O., and Huber, R. (1991) *EMBO J. 10*, 1997.
48. Siddiqui, A. S., and Barton, G. J. (1995) *Protein. Sci. 4*, 872−884.
49. Houry, W. A., Rothwarf, D. M., and Scheraga, H. A. (1994) *Biochemistry 33*, 2516−2530.
50. Touchette, N. A., Perry, K. M., and Matthews, C. R. (1986) *Biochemistry 25*, 5445−5452.
51. Jonsson, T., Waldburger, C. D., and Sauer, R. T. (1996) *Biochemistry 35*, 4795−4802.
52. Walkenhorst, W. F., Green, S. M., and Roder, H. (1997) *Biochemistry 36*, 5795−5805.
53. Sauder, J. M., MacKenzie, N. E., and Roder, H. (1996) *Biochemistry 35*, 16852−16862.

BI972936Z